Sedimentary Geology 425 (2021) 106021

Contents lists available at ScienceDirect

Sedimentary Geology

journal homepage: www.elsevier.com/locate/sedgeo

Facies stacking and distribution in the Gabbs Formation (Late Triassic, west-Central Nevada, U.S.A.): An environmental baseline to the end-Triassic carbonate crisis

Annaka M. Clement *, Lydia S. Tackett

North Dakota State University, Department of Geosciences, Fargo, ND 58108, USA

ARTICLE INFO

Article history:
Received 8 August 2021
Received in revised form 10 October 2021
Accepted 12 October 2021
Available online 16 October 2021

Editor: Dr. Jasper Knight

Keywords:
Triassic/Jurassic boundary
Facies
Carbonate ramp
Mixed systems
Sequence stratigraphy
Panthalassa

ABSTRACT

The primarily carbonate Gabbs Formation of west-central Nevada, U.S.A., remains an important, rare example of Panthalassan shallow-marine environments from the Late Triassic and through the Triassic–Jurassic boundary. Its relevance as a locality persists, particularly as the end-Triassic mass extinction interval is increasingly recognized as a carbonate crisis, evidenced by the global decline of carbonate facies and calcareous marine organisms. However, important transitions across key stratigraphic boundaries in this region have tended to be evaluated in isolation, producing an incomplete picture of sedimentation through the duration of the Late Triassic leading up to the geochemical crises and mass extinction at the close of the Triassic. In this work, multiple correlative measured sections are used to describe the facies in the mixed carbonate-siliciclastic ramp and characterize controls on carbonate facies. The outer ramp transition to inner ramp facies of the Gabbs represent a transgressive–regressive–transgressive cycle culminating in a transition to terrigenous inputs and a gradual decline of carbonate sediments stratigraphically below the mass extinction interval. This predictable loss of carbonate facies and the near continuous deposition of the Gabbs Formation allow for evidence of facies changes and acidifying conditions in the latest Triassic to be considered independently, in contrast to other global Late Triassic sections where depositional hiatuses or abrupt facies changes often compound these records. Establishing a baseline sedimentation for the Late Triassic demonstrates that the final loss of carbonate facies can be decoupled from the onset of acidifying conditions, resulting in a more precise timeline of latest Triassic environmental upheaval.

1. Introduction

The Gabbs Formation, west-central Nevada, U.S.A., comprises abundant and accessible Late Triassic-age marine deposits containing diverse fauna that record transitions in the paleoecological communities prior to the end-Triassic mass extinction (Laws, 1982; Taylor et al., 2000; Tackett and Bottjer, 2016). The Gabbs Formation also contains a key marine exposure of the Triassic–Jurassic boundary for the Western United States. The complete section in Muller Canyon spans the boundary with no evidence of a hiatus, a feature that is rare for primarily carbonate global boundary sections that normally record a depositional hiatus or highly condensed section (Hallam and Wignall, 2000; Lucas et al., 2007; Ward et al., 2007; Guex et al., 2009; Greene et al., 2012; Korte et al., 2018). Owing to its completeness, the Muller Canyon exposure was a previous candidate for the Hettangian GSSP (Lucas et al., 2007; Ward et al., 2007). However, the stratigraphic interval containing faunal transitions within the Gabbs Formation is not exposed in Muller Canyon. Few studies have considered faunal and facies changes in the mass extinction interval and at the Triassic–Jurassic boundary within the broader context of faunal, facies, and paleoecological shifts recorded in the lower portions of Gabbs Formation found outside of Muller Canyon. While this is a somewhat unique feature of the Gabbs Formation exposures, the piecemeal view of its stratigraphy is non-trivial as the section in Muller Canyon, owing to its relative accessibility and many geochemical studies (Guex et al., 2004; Ward et al., 2007; Guex et al., 2009; Thibodeau et al., 2016), is almost exclusively what is compared to global end-Triassic extinction and Triassic–Jurassic boundary sections. This creates a superficial disconnect between the lower facies and paleoecological shifts not exposed in Muller Canyon, and the facies changes, geochemical excursions, and extinction event that are expressed.

The disconnect between the study areas of the facies and the lack of correlative sections used to confirm facies relationships are particularly problematic for analysis of the extinction and other Late Triassic faunal changes. Mass extinctions are recognized by the permanent disappearance of existing taxa in the context of the paleoenvironment they occupied. Work over the last 30 years incorporating fossil ranges into sequence stratigraphic contexts has highlighted and codified the importance of facies control in apparent extinction events (Patzkowsky and Holland, 2012; Holland, 2020). Multiple facies in the Gabbs Formation

* Corresponding author.
E-mail address: annaka.clement@ndsu.edu (A.M. Clement).

https://doi.org/10.1016/j.sedgeo.2021.106021
0037-0738/

are characterized by distinct fossil assemblages whose stratigraphic changes are unlikely to be related to the possible global warming and ocean acidification related to the main phase of Central Atlantic Magmatic Province (CAMP) volcanism in the latest Triassic (Muller and Ferguson, 1939; Laws, 1978, 1982; Hallam and Wignall, 2000). Therefore, in order to understand the faunal and sedimentological changes that occurred in the latest Triassic at this important locality, a clear definition of members and facies in the Gabbs Formation is critical. Previous work documenting facies transitions and faunal assemblages characterized the Gabbs Formation with well-exposed sections that distinctly show a given facies. However, sections featured exhibit only minimal overlap and rarely include the Muller Canyon section (Muller and Ferguson, 1936, 1939; Laws, 1978, 1982; Taylor et al., 1983; Hallam and Wignall, 2000) (Fig. 1), in contrast to recent studies of the post-extinction Sunrise Formation (Ritterbush et al., 2014, 2016; Clement et al., 2020). No unified depositional model has been described for the facies changes observed in Muller Canyon (near the proposed Triassic–Jurassic GSSP) and those facies expressed in underlying strata (studied elsewhere in the vicinity of New York Canyon). Rarely have these changes been considered across the exposure area of the Gabbs Formation in the New York Canyon area, leading to discrepancies in member definitions and uncertainty over the spatial component of facies changes.

The approach in this paper uses multiple localities with equivalent sections that cover the entire Gabbs Formation (Fig. 1) and applies principles of sedimentology and sequence stratigraphy, in concert with a new, detailed map of the region, and updated descriptions of the Gabbs members. This approach establishes more robust and generalized descriptions of the named members and characterizes the temporal and spatial variation among facies in the New York Canyon area. This treatment of the Gabbs Formation then provides a framework in which faunal and ecological changes in the Late Triassic can be assessed and be more directly related to significant events at around the Triassic–Jurassic boundary. Within this framework, the unique completeness of the latest Triassic deposits of the Gabbs Formation provides a valuable opportunity to study the timing of faunal, ecological, and facies changes in relation to evidence of global acidification and perturbations in the carbon cycle. This more complete characterization of the carbonate system of the Gabbs Formation may then serve as a baseline when considering the acidification event immediately prior to the Triassic–Jurassic boundary and the return to a carbonate depositional system in the Early Jurassic with significantly different faunas.

2. Geologic setting

The limestone deposits of the Late Triassic Gabbs Formation are interpreted to have accumulated in a back-arc basin on the western margin of Pangea with a volcanic arc to the west (Speed, 1978; Reilly et al., 1980; Oldow, 1984). The Gabbs Formation was originally defined by Muller and Ferguson (1936) in its type locality in New York Canyon, southeast of Volcano Peak, in the southern Gabbs Valley Range, Nevada, U.S.A. (Figs. 2, 3). It was also recognized in the Gillis Range, Garfield Hills, Paradise Range and Shoshone Mountains, though not differentiated from the Jurassic Sunrise Formation (Muller and Ferguson, 1936, 1939; Ferguson and Muller, 1949) (Fig. 2). Given the limited geographic extent of the Gabbs Formation, interpretations of basin type and geometry are based on the underlying Luning Formation, which is much thicker, widespread, and has abundant exposures across several ranges (Speed, 1978; Reilly et al., 1980; Oldow, 1984). Western and northern exposures of the Luning Formation are considered more basin-central than deposits to the southeast (including the New York Canyon area) based on the presence of basinal facies and sandstones with a more significant volcanic provenance (Reilly et al., 1980; Oldow, 1984). This original northwest basin–southeast shore orientation of basin dip in the Luning Formation indicates that the Gabbs Formation also likely

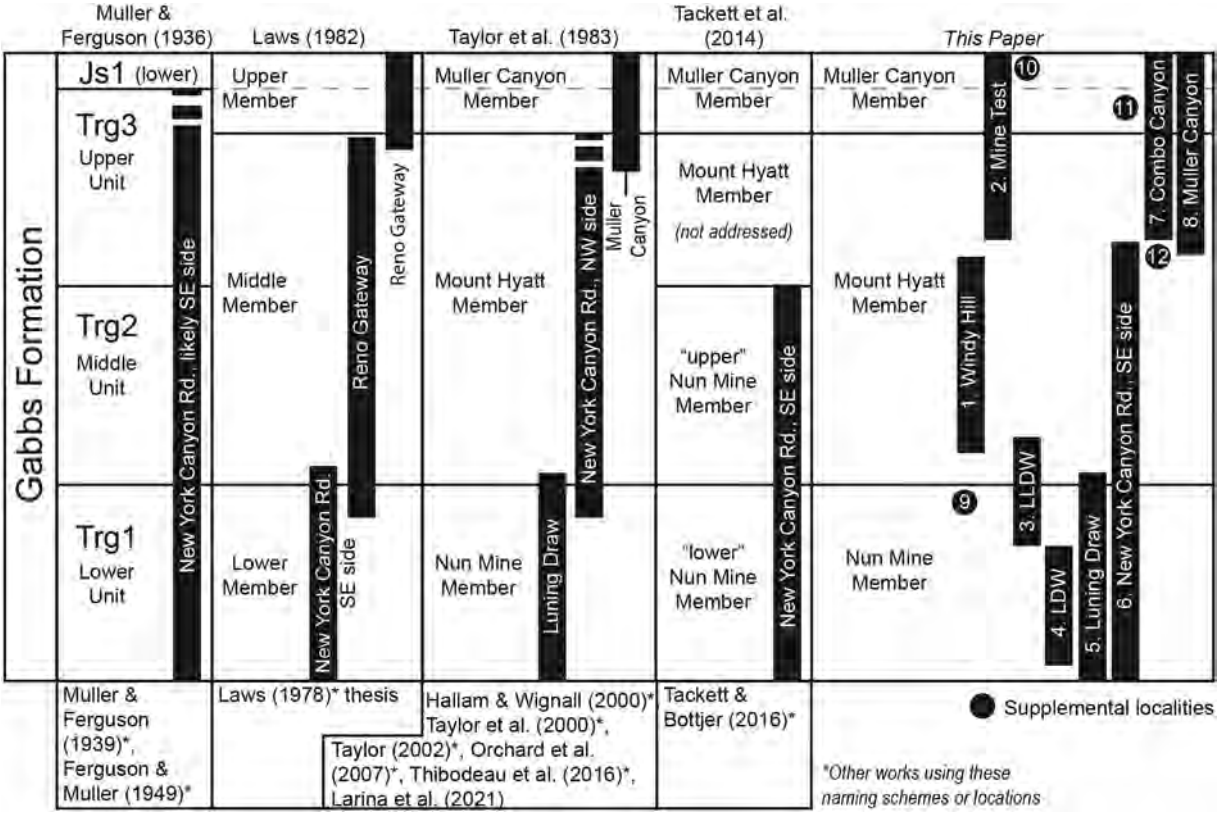

Fig. 1. Comparison chart of subunits described in the Gabbs Formation. Comparison of the described subunits and localities used by previous authors. This work uses multiple measured sections and supplemental localities to describe each member and facies of the Gabbs Formation in order to perform a sequence stratigraphic analysis.

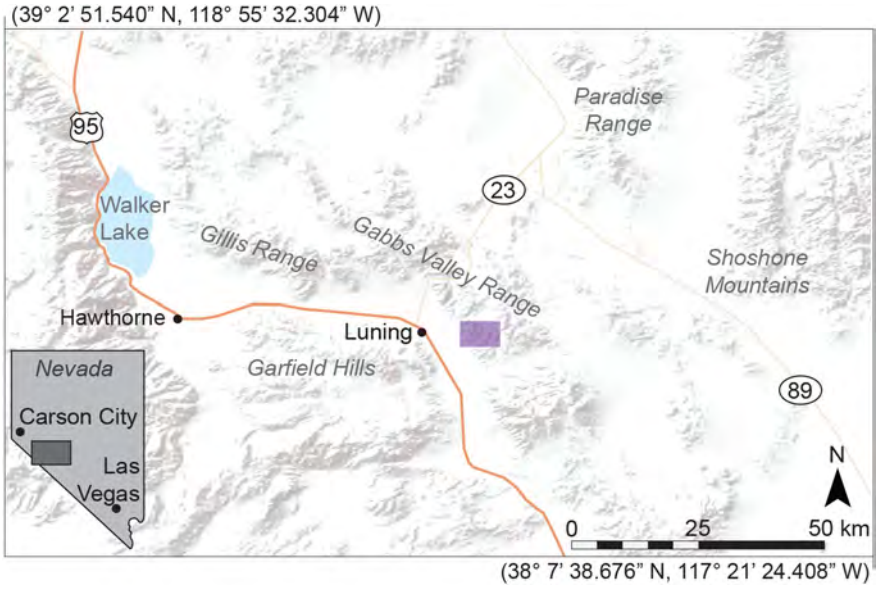

Fig. 2. Regional map of ranges containing the Gabbs Formation. Map area is indicated by the dark gray box on the state of Nevada outline. Labeled ranges contain the Gabbs Formation, occurring with the Sunrise Formation in all ranges except the Gabbs Valley Range. Purple box in the Gabbs Valley Range indicates the area of the geologic map (Fig. 3) and includes the type localities of the Gabbs Formation. Map area: northwest corner (39° 2′ 51.540″ N, 118° 55′ 32.304″ W), southeast corner (38° 7′ 38.676″ N, 117° 21′ 24.408″ W).

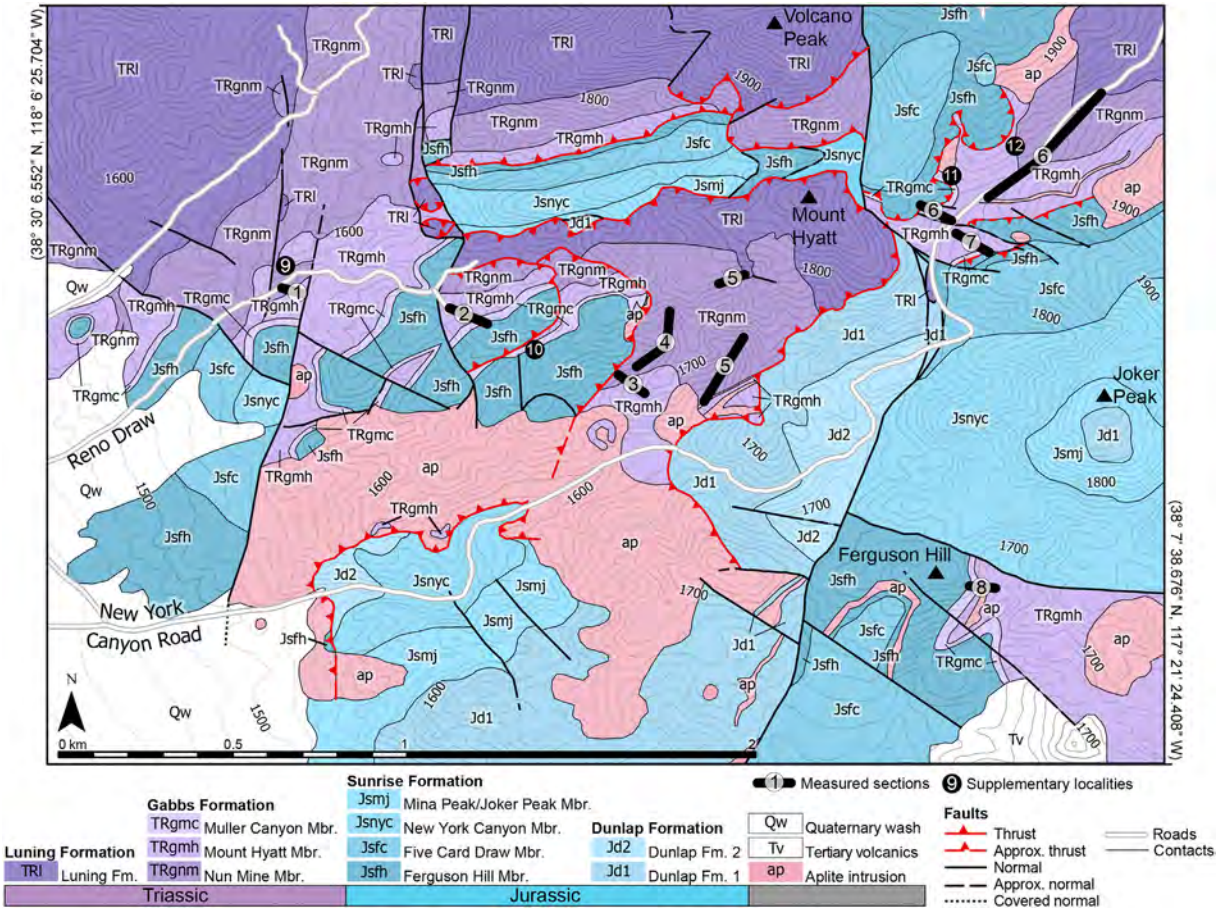

Fig. 3. Geologic map of the New York Canyon area of the Gabbs Valley Range, Nevada, U.S.A. Geologic map is based on Ferguson and Muller (1949) as well as field observations and satellite imagery. This map is geolocated and produced using ArcGIS Pro. Topographic lines are produced using the USGS 10 m resolution digital elevation models (U.S. Geological Survey, 2017). Map area: northwest corner (38° 30′ 6.552″ N, 118° 6′ 25.704″ W), southeast corner (38° 28′ 56.280″ N, 118° 4′ 41.916″ W). Other file-types are available with archived data at http://dx.doi.org/10.17632/36wbbhkc3v.1.

accumulated on the western margin of Pangea, in the landward portion of the back-arc basin.

In the vicinity of New York Canyon, the Gabbs Formation is divided into three members: the Nun Mine Member, Mount Hyatt Member, and Muller Canyon Member (Taylor et al., 1983). The lower Nun Mine Member conformably overlies the Norian-age Luning Formation and contains interbedded purplish shale and limestone. The Nun Mine Member also hosts the lower fossil assemblage (*Cochloceras* Association) described by Muller and Ferguson (1936, 1939) and Laws (1978, 1982) containing primarily *Cochloceras fisheri* (corrected to *Paracochloceras nunminensis* by Taylor et al. (2021)) and *Rhabdoceras suessi* with rare *Nuculana* and *Myophoricardium*. The middle Mount Hyatt Member is primarily limestone with minor shale and contains the middle and upper fossil assemblage described from Muller and Ferguson (1936, 1939) and Laws (1978, 1982). The middle fossil assemblages of Laws (1978, 1982) include the *Plicatula* Association (containing hyperabundant *Plicatula perimbricata* and common *Tutcheria*, *Arcavicula*, and *Arcestes*) and the *Tutcheria* Association (containing abundant *Tutcheria* and *Cassianella* and a diverse array of bivalves and brachiopods). The upper fossil assemblage of the Mount Hyatt Member is the *Nuculoma* Association (containing primarily *Nuculoma* and other burrowing bivalves) (Laws, 1978, 1982). The paleoecology of the middle and upper assemblages from a site in New York Canyon is detailed in Tackett and Bottjer (2016). The upper Muller Canyon Member conformably underlies the early Jurassic-age Sunrise Formation (Muller and Ferguson, 1936; Laws, 1982; Taylor et al., 1983) and is defined as the uppermost approximately 15 m of the Gabbs Formation where siltstones are the dominant lithology. The Muller Canyon Member contains the Triassic–Jurassic boundary, distinguished based on biostratigraphy (Muller and Ferguson, 1936; Laws, 1978, 1982; Taylor et al., 1983; Guex et al., 2004; Ward et al., 2007). The highly studied exposure of the Muller Canyon Member in Muller Canyon also contains the initial negative $\delta^{13}C$ excursion (ICIE) that is considered coincident with the mass extinction and acidifying conditions at the end of the Triassic and is commonly used to correlate global localities (Guex et al., 2004, 2009; Ward et al., 2007; Thibodeau et al., 2016; Korte et al., 2018).

3. Methods

Eight stratigraphic sections of the Nun Mine Member, Mount Hyatt Member, and Muller Canyon Member of the Gabbs Formation were measured in the vicinity of New York Canyon in the Gabbs Valley Range east of Luning, Nevada (Figs. 1–3). An additional four outcropping localities were used as supplemental sites, which have limited exposure or lack clear membership boundaries or stratigraphic tie-points, but still provide additional information on facies or biostratigraphy (Figs. 1, 3; sites 9–12). The stratigraphic sections are exposed on several adjacent thrust sheets (Ferguson and Muller, 1949), producing a modern transect of 3.86 km; however, the original distance and spatial orientation of the sections were likely different prior to faulting (Oldow, 1984). In each section the lithology, bedding, sedimentary structure, contacts, and fossils were described to determine depositional environments and to define facies. Carbonate lithology was determined using the modified Dunham Classification system (Dunham, 1962; Embry and Klovan, 1971). Comparative petrographic thin sections were made from hand samples representing depositional environments from multiple columns to aid lithologic description, facies identification, and correlation. The facies and their associations were used to develop a facies model based on Waltherian relationships. The eight stratigraphic sections were assembled into a stratigraphic cross-section and correlated based on facies and stacking patterns. A full sequence stratigraphic interpretation was not possible owing to the limited extent of the Gabbs Formation that each measured section provided. Sequence stratigraphic principles were used to identify potential significant surfaces, sedimentation patterns, and facies relationships.

The composition and microstructure of select samples were analyzed in thin sections and by X-ray diffraction. Mineral identification and approximate composition of thin sections were done on a Zeiss Discovery.V12 with the Zeiss Zen Pro software and imaging.

X-ray diffraction was carried out on samples of fine-grained and fissile facies using a Bruker D8 Discovery X-ray diffractometer. Samples were hand-ground to a powder of approximately 5 micron grain size, spiked with approximately 10% ZnO as an internal standard, and smear-mounted to glass slides. The Bruker D8 was run with a Copper Ka source with wavelength 1.5406 Å at 40 kV and 40 mA. A 100 micron collimator was used on the beam, and the sample was rotated about the z-axis while oscillating (1 mm amplitude) in x and y directions producing a 2 mm circle-shaped scan area. Scans were produced in 5 steps of width 15 degree 2-theta from 15 to 75 degree 2-theta at 400 s per step. Scans were integrated into profiles and analyzed in the Bruker DIFFRAC.EVA software.

An updated geologic map was produced in ArcGIS Pro for the New York Canyon area, including Muller Canyon, covered by Ferguson and Muller (1949). A detailed description of the changes made to the updated map can be found in Supplementary document 1.

4. Results

4.1. Facies of the Gabbs Formation

A total of six facies of the Gabbs Formation were observed in the New York Canyon region. Facies were defined by a distinct set of characteristics including lithology, bedding, sedimentary structure, fossils, and contact relationships to other facies (Table 1). Measured sections were colored according to facies and arranged into a cross-section (Fig. 4). A larger version of this cross-section is available at http://dx.doi.org/10.17632/36wbbhkc3v.1. The facies of the Gabbs Formation are interpreted to represent environments along a mixed carbonate-siliciclastic ramp including outer ramp, mid-ramp, and distal inner ramp environments. A revised description of the Gabbs Formation members and their constituent facies can be found in Supplementary document 2.

4.1.1. Calcareous shale (CS)

The calcareous shale facies (CS) is composed of purple–gray, and occasionally red, carbonate-containing shale. Mineralogy from X-ray diffraction consists of calcite, quartz, muscovite, and illite-group minerals (Fig. 5). Quartz grains are not visible in hand sample. Facies CS is thin to medium-bedded (3–30 cm) but weathers readily to slopes that obscure bedding and give the appearance of more massive intervals of calcareous shale. In this work no macrofossils were found in the calcareous shale facies. Facies CS had gradational contacts and is commonly interbedded with facies PLM. Bedding is very thin to medium but is often obscured by weathering. Bedding is best expressed in well-exposed sections such as Luning Draw and Luning Draw West (Fig. 6A). Facies CS conformably underlies and is typically interbedded with facies PLM.

4.1.2. Purple lime mudstone (PLM)

The purple lime mudstone (PLM) facies is composed of dark gray lime mudstone that weathers to a purple color and often to a fissile shaly texture. Petrographically, facies PLM is composed of silt and micrite with rare small and micritized shell fragments (Fig. 7A). Some beds contain rare silt to fine sand-sized rounded grains of calcite. Facies PLM is thin to medium-bedded (3–30 cm), with occasional thick (30–100 cm) beds, and often medium to thickly laminated (0.3–1 cm). Laminations are commonly wavy (Fig. 6A). Bedding and lamination are frequently obscured by weathering and are best expressed in sections such as Luning Draw (Fig. 6A) and Luning Draw West. Fossils are rare in the purple calcareous mudstone and when present include demersal ammonites (commonly *Rhabdoceras* and *Paracochloceras*), unknown pelagic ammonites, and rare bivalves, corresponding to Laws (1978, 1982) *Cochloceras* Association. Facies PLM is often interbedded with the calcareous shale facies and has a

Table 1
Facies of the Gabbs Formation descriptions and characteristics including proposed depositional environment.

Facies	Lithology	Mineralogy/petrography	Bedding & sedimentary structures	Fossils	Contacts	Depositional setting
Calcareous shale (CS)	Purple–gray and occasionally red carbonate containing shale. Weathers readily	Mineralogy from X-ray diffraction consists of calcite, quartz, muscovite, and illite-group minerals (Fig. 5). Quartz grains are not visible in hand sample.	Thin–medium (3–30 cm), but weathers readily to slopes that obscure bedding and give the appearance of more massive intervals.	No fossils have been found in this work	Conformably underlies and is often interbedded with facies PLM.	Outer ramp transition
Purple lime mudstone (PLM)	Dark gray lime mudstone that weathers purple. Beds weather readily to a fissile shaley texture.	Carbonate silt and micrite with rare small and micritized shell fragments (Fig. 7A). Some beds contain rare silt to fine sand-sized rounded grains of calcite.	Thin–medium (5–30 cm), occasionally thick. Often displaying medium–thick wavy laminae (Fig. 8A). Rare bedding planes preserve *Thalassinoides* burrows	Common *Paracochloceras* and *Rhabdoceras* and rare large pelagic ammonites on bedding planes. Rare bivalves.	Sharply, but conformably overlies the Luning Formation dolostone. Interbedded with facies CS. Gradationally underlies facies SPF.	Outer ramp transition
Skeletal packstone–floatstone (SPF)	Gray skeletal packstone to floatstone with visible fine sand-sized carbonate grains. In hand sample, facies SPF beds are more visibly grainy than the purple lime mudstone facies and contain a range of large skeletal clasts from 0 to 20%. Weathers to a tan color similar to facies HSP (Fig. 6B).	Matrix supported carbonate with 0–20% whole and partial large skeletal bioclasts. Matrix is silt to very fine sand-sized with many matrix grains of biogenic origins including weathered fossils and rare to common coated grains and peloids (Fig. 7B, C).	Thin–thick (5–100 cm), most commonly packstone thin–medium (5–30 cm) and floatstone medium–thick (20–50 cm) Occasional small (<10 mm) *Skolithos*.	Fossil fragments appear commonly as sand-sized grains. Samples with at least 10% large skeletal grains contain abundant whole and partial bivalves and unidentifiable stereom fragments. Rare ammonites, gastropods, and sponge spicules.	Sharply, but conformably, overlies facies PLM and gradationally underlies facies HSP and SLMW.	Mid-ramp
Hashy skeletal packstone (HSP)	Skeletal packstone with fragmentary and often hashy bioclasts in a silt to fine sand-sized carbonate matrix. Similarly resistant and tan weathering to facies SPF (Fig. 6B).	Bioclast-supported carbonate with abundant small, fragmentary, and hashy skeletal grains in a silt to fine sand-sized carbonate matrix. Matrix grains are primarily composed of fragmentary and rounded biogenic carbonate (Fig. 7D, E). Skeletal clasts include abundant fragmentary mollusks and echinoderm stereom. Fine, angular to subangular quartz grains are rare but present in most thin sections (Fig. 7D, E).	Thin–medium (5–20 cm)	Abundant fragmentary mollusks and echinoderms including crinoid columnals, echinoid spine fragments, and fragmentary stereom.	Gradationally overlies facies SPF. Sharply underlies facies SLMW.	Mid-ramp
Silty lime mudstone–wackestone (SLMW)	Dark gray micrite with <10% skeletal bioclasts. May appear slightly silty in hand sample. Weathers brown to gray in outcrop (Fig. 6C). May effervesce less readily in the presence of HCl depending on the amount of quartz silt. Silty tops of beds tend to be pink in color.	Carbonate rock with less than or equal to 10% skeletal bioclasts, primarily composed of carbonate mud and silt with at least 1% silt-very fine sand lower sized grains of angular-subangular quartz (Fig. 7F, G). The tops of beds tend to contain a higher percentage of quartz silt.	Thin–thick (most commonly 10–40 cm), commonly planar or cross laminated at the tops of beds (Figs. 7F, 8B) Common small (<10 mm) *Skolithos* and cf. *Palaeophycus*	Rare whole small burrowing bivalves, and rare fragmentary echinoderms. Lamination on the tops of beds commonly interrupted or obscured by bioturbation. Commonly, small vertical burrows are visible in cross section and branching planar burrows are exposed on bedding planes.	Commonly interbedded with facies SW lower in columns where it is found, and interbedded with calcareous siltstone facies higher in columns where it is found (Fig. 6C–D).	Inner ramp transition
Calcareous siltstone (CSt)	Brown to pinkish beds of silt-sized siliciclastic grains with a variable amount of carbonate matrix and cement.	Grains are dominantly silt-sized with minor very fine, subrounded–subangular grains (Fig. 7H, I). Primarily quartz with minor amounts of chert lithic grains and lithic grains composed of fine groundmass. Opaque oxide grains well-distributed in thin sections. Opaque, organic-rich, matrix material between grains common. Mineral composition by X-ray diffraction includes quartz, calcite, plagioclase feldspar, and illite-group minerals (Fig. 5).	Thin–medium (5–20 cm), bedding planes often difficult to differentiate, giving the appearance of thick to massive bedding. Commonly planar and cross-laminated (Fig. 8C). Common cf. *Palaeophycus*	No body fossils were observed in this facies from this work; however, rare ammonites and bivalves have been previously reported (Ward et al., 2007; Taylor et al., 2021).	Gradationally overlies facies SLMW and is commonly found interbedded with facies SLMW (Fig. 6C–E).	Inner ramp

sharp but conformable contact with the skeletal packstone–floatstone facies. In well-exposed sections (Fig. 4; measured sections 3–5), purple lime mudstone is the dominant lithology of the interbedded intervals of facies CS and PLM and tends to increase up-section. In weathered sections (Fig. 4; measured section 6), facies PLM appears as the minor lithology and exposures are dominated by the calcareous shale facies (CS). This may be a

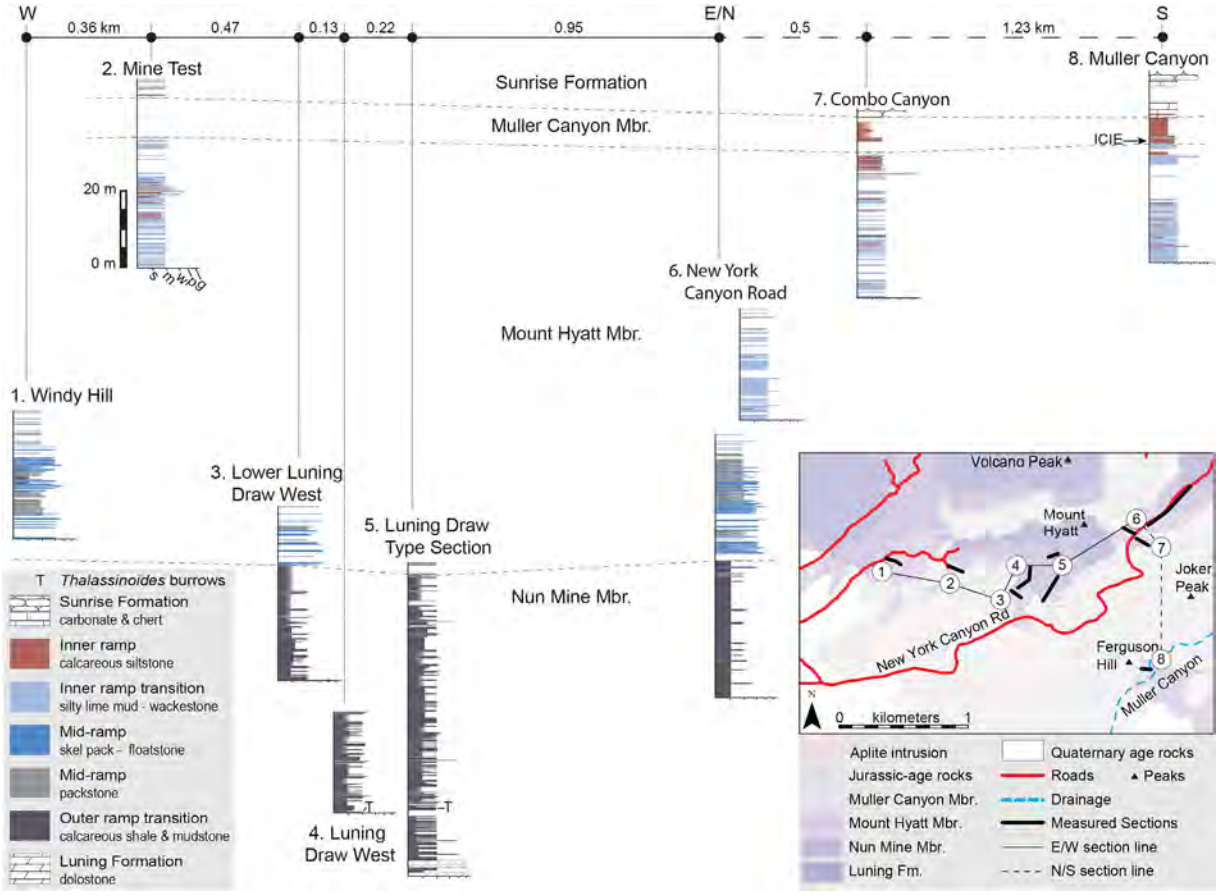

Fig. 4. Cross-section of measured sections of the Gabbs Formation. ICIE marks the position of the initial carbon isotope excursion in Muller Canyon (Guex et al., 2004; Ward et al., 2007; Thibodeau et al., 2016; Larina et al., 2021). Larger cross section and multiple file formats available with archived data at http://dx.doi.org/10.17632/36wbbhkc3v.1.

result of extensive weathering of the purple lime mudstone facies such that it does not outcrop well and is unable to be differentiated from facies CS on weathered slopes.

4.1.3. Skeletal packstone–floatstone (SPF)

Skeletal packstone–floatstone (SPF) beds range from packstone beds, composed of silt to fine sand-sized, grain-supported gray carbonate with a lime mud matrix, to beds of floatstone resembling the packstone beds and additionally containing 10–20% large skeletal bioclasts, whole and fragmentary. Petrographic analysis revealed the silt–very fine sand-sized grains in both packstone and floatstone beds are primarily biogenic including weathered fossils and rare to common coated grains and peloids (Fig. 7B, C). Large fossil bioclasts in floatstone intervals include abundant bivalves and rare ammonites, gastropods,

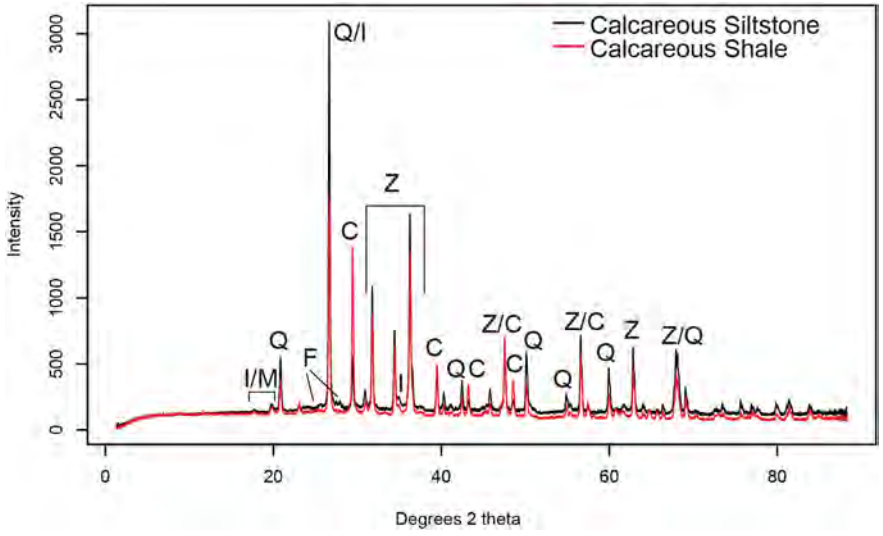

Fig. 5. X-ray diffraction patterns for samples from the calcareous shale facies (CS) and calcareous siltstone facies (CSt). Indicative peaks or regions are marked for primary minerals. Z: zincite, added as an internal standard; Q: quartz; C: calcite; I: illite group minerals; M: muscovite; F: plagioclase feldspar.

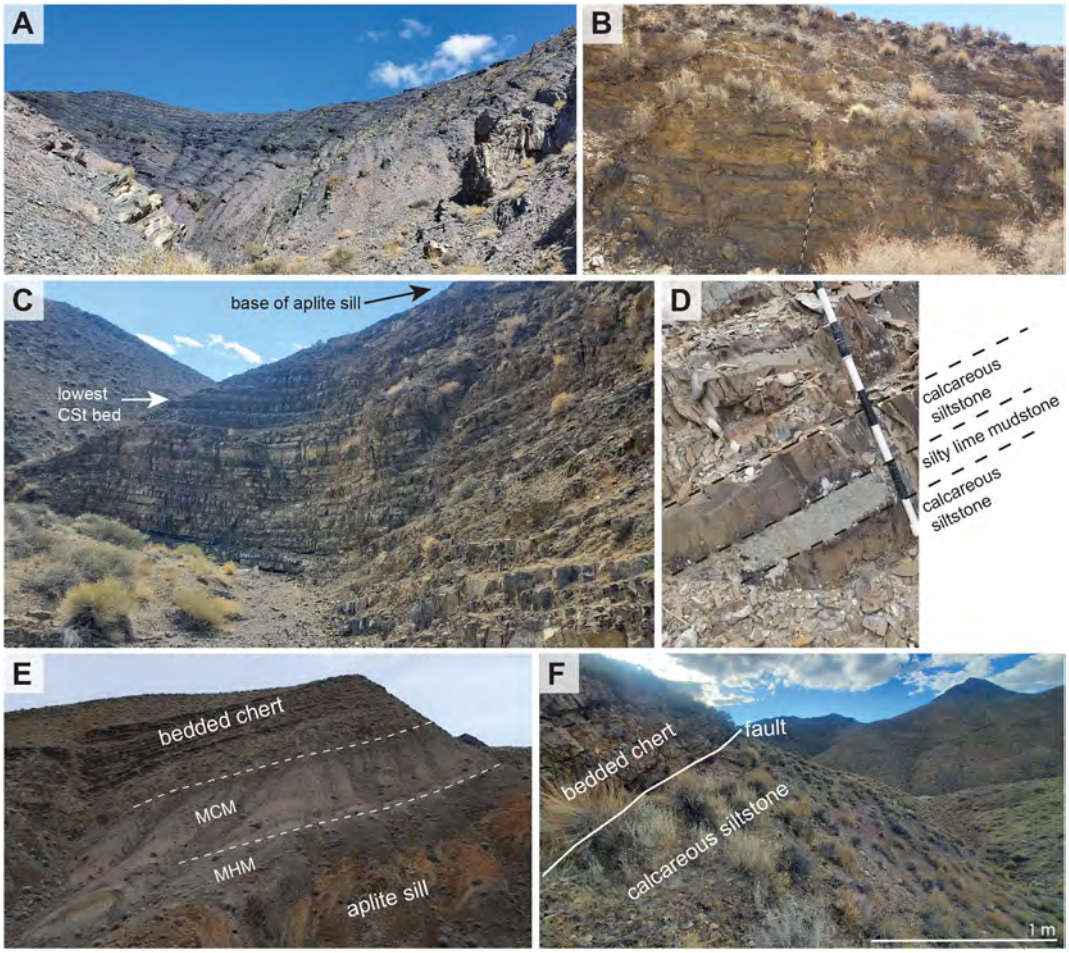

Fig. 6. Field photographs of Gabbs Formation Members. (A) View of the Nun Mine Member type section (column 5, Figs. 2 and 6) containing interbedded calcareous siltstone (CS) and purple lime mudstone (PLM) facies in Luning Draw looking down-section approx. north–northeast. (B) Representative outcrop of the Mount Hyatt Member containing skeletal packstone–floatstone (SPF), and hashy skeletal packstone (HSP) facies. Outcrop located on the southeast side of New York Canyon Road (Figs. 3, 4; measured section 6). (C) Lower portion of the measured section in column Muller Canyon containing silty lime mudstone–wackestone (SLMW) and calcareous siltstone (CSt) facies (Figs. 3, 4; measured section 8). Direct label indicates the position of the lowest bed of calcareous siltstone facies (10.6 m above the canyon floor, meter 14.7 in the measured section); above this silty lime mudstone–wackestone and calcareous siltstone facies are interbedded. Direct label indicates the base of an aplite sill that intrudes the upper Mount Hyatt Member. View is looking south down Muller Canyon. (D) Interbedded silty lime mudstone–wackestone and calcareous siltstone facies near the top of the Mount Hyatt Member from Mine Test (Figs. 3, 4; measured section 2) meter 21. (E) View of the type locality of the Muller Canyon Member (Figs. 3, 4; measured section 8) on Ferguson Hill looking north, courtesy of Dr. Kathleen Ritterbush. Directly labeled aplite sill is the same as the one indicated in (C). Approximately 8 m of Mount Hyatt Member (MHM) are partially exposed above the aplite sill. Dashed lines indicate the base and top of the Muller Canyon Member (MCM). The bedded chert at the top of Ferguson Hill is part of the Ferguson Hill Member of the Sunrise Formation. (F) Top of the Muller Canyon Member truncated by a thrust fault in Combo Canyon (Figs. 3, 4; measured section 7). The trust fault juxtaposes the calcareous siltstone of the Muller Canyon Member and the bedded chert of the Sunrise Formation. The Triassic–Jurassic boundary may be faulted-out at this locality and in much of the northeast area of New York Canyon (Fig. 3).

echinoderms, and brachiopods. Similar to previous studies (Muller and Ferguson, 1939; Laws, 1978, 1982; Tackett and Bottjer, 2016), *Cassianella*, *Tutcheria*, and cf. *Plicatula* were abundant and other bivalve taxa including *Schafhaeutlia*, *Limatula*, *Chlamys*, and *Frenguelliella* were common. Floatstone intervals of facies SPF often contain very fine quartz sand grains that are notably absent from facies PLM and CS. Facies SPF is thin to thickly bedded (3–100 cm), though packstone intervals tend to be thin to medium bedded (most commonly 5–30 cm) and floatstone typically medium to thickly bedded (most commonly 20–50 cm). Wavy bedding planes are common in facies SPF. In outcrop, facies SPF beds show a distinct tan–brown weathering and are more resistant than beds of facies PLM (Fig. 6B). Facies SPF sharply but conformably overlies facies PLM and gradationally underlies facies HSP and SLMW.

4.1.4. Hashy skeletal packstone (HSP)

The hashy skeletal packstone facies (HSP) is composed of bioclast-supported carbonate with abundant small, fragmentary, and hashy skeletal grains in a silt to fine sand-sized carbonate matrix. Petrographic analysis showed matrix grains are primarily composed of fragmentary and rounded biogenic carbonate (Fig. 7D, E). Skeletal clasts include abundant fragmentary mollusks and echinoderm stereom. Fine, angular to subangular quartz grains are rare but present in most thin sections (Fig. 7D, E). Facies HSP is thin to medium-bedded (5–20) and in outcrop its resistant beds weather tan, similar in appearance to facies SPF (Fig. 6B). Facies HSP displays sharp lower contacts with the facies SPF.

4.1.5. Silty lime mudstone–wackestone (SLMW)

The silty lime mudstone–wackestone facies (SLMW) is composed of dark gray carbonate rock with <10% skeletal bioclasts in a matrix of carbonate mud and silt with at least 1% silt to very fine lower sand-sized grains of angular to subangular quartz (Fig. 7F, G). In outcrop, this facies can be difficult to distinguish owing to its resemblance to facies SPF. Facies SLMW may effervesce less readily in the presence of HCl depending on the amount of quartz silt. Facies SLMW typically contains smaller burrowing bivalves, notably cf. *Nucula*, *Palaeonucula*, *Plagiostoma*, *Frenguelliella*, and myophoriids corresponding to Laws (1978, 1982) *Nuculoma* Association.

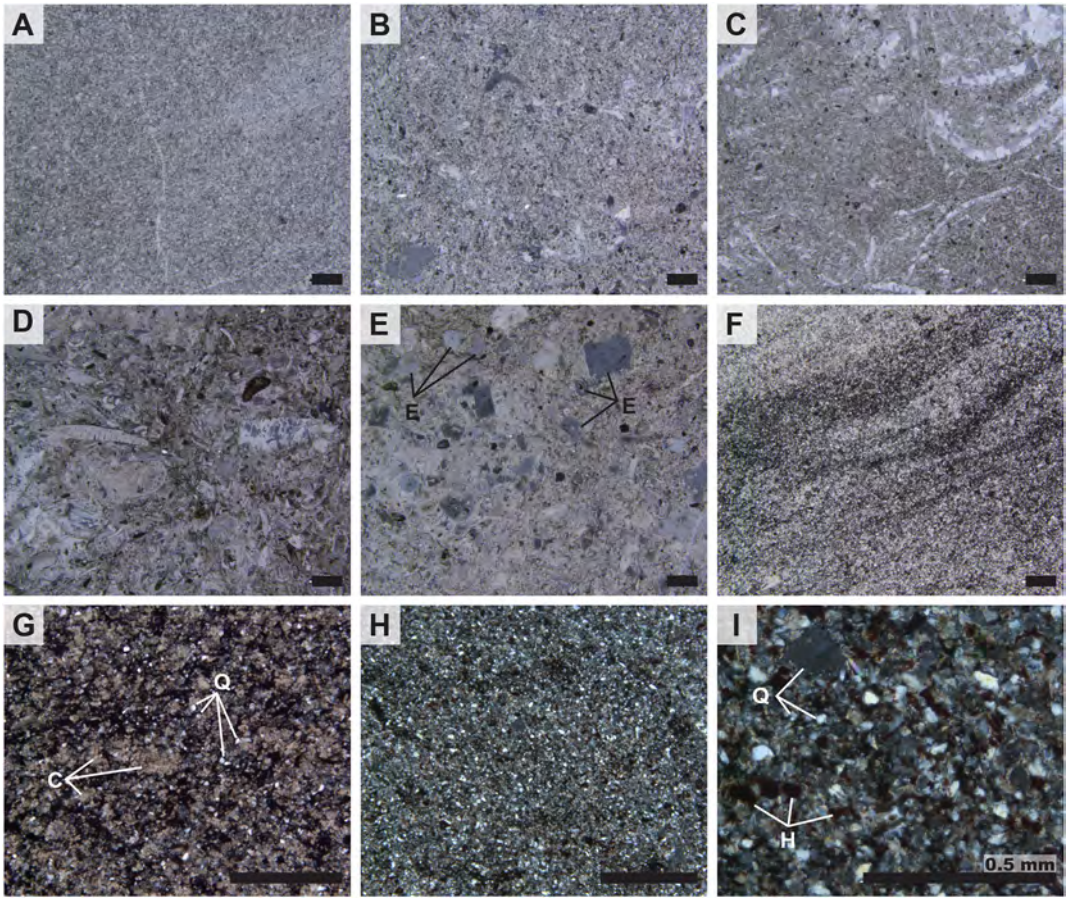

Fig. 7. Thin sections of Gabbs Formation facies. All photomicrographs are in cross-polar light. All scale bars 1 mm unless otherwise indicated, column refers to measured sections in Fig. 2, meterage from Fig. 6. (A) Mudstone interpreted to be purple lime mudstone facies. Sample from column 5. Luning Draw Type Section meter 76.45. (B) Bioclastic packstone interpreted to be from skeletal packstone–floatstone facies. Sample from column 6. New York Canyon Road meter 43.6. (C) Skeletal floatstone interpreted to be from skeletal packstone–floatstone facies. Sample from column 3. Lower Luning Draw West meter 31.3. (D) Skeletal packstone containing bivalve fragments and stereom interpreted to be from hashy skeletal packstone facies. Sample from column 6. New York Canyon Road meter 53.2. (E) Skeletal packstone containing primarily echinoderm stereom (labeled E) interpreted to be from facies hashy skeletal packstone facies. Sample from column 6. New York Canyon Road meter 56.95. (F) Silty mudstone with cross-laminae interpreted to be from silty lime mudstone–wackestone facies. Sample from column 8. Muller Canyon meter 7.95. (G) Higher magnification of silty mudstone from (F). Q: examples of quartz silt grains, C: examples of carbonate mud. (H) Calcareous siltstone interpreted to be form facies calcareous siltstone facies. Sample from supplementary locality 11. Hidden Valley (HV AC 218). (I) Higher magnification of (H) showing grain morphology and mineralogy. Subangular to subrounded quartz silt grains with carbonate cement. Q: examples of quartz silt grains. H: hematite grains.

The skeletal grains in facies SLMW tend to be whole and frequently articulated small burrowing bivalves. Silty lime mudstone–wackestone facies is thin to thickly bedded (typically 10–40 cm) and commonly displays planar or cross-laminations (Figs. 7F and 8B) near the tops of beds. The top 5 cm of SLMW beds frequently contains up to 50% quartz silt, appears more pinkish-brown, and commonly displays bioturbation. Bioturbation frequently obscures laminations and presents as small (<1 cm diameter) *Skolithos* in cross-section and dense cf. *Palaeophycus* on some exposed bedding planes. Facies SLMW is commonly interbedded with facies SPF lower in measured sections Windy Hill and New York Canyon Road, and interbedded with calcareous siltstone facies higher in measured sections Mine Test, Combo Canyon, and Muller Canyon (Figs. 4 and 6C, D). The increase in terrigenous content in the tops of beds of facies SLMW indicates that facies SLMW may grade vertically into facies CSt, though the boundaries appear sharp when observed interbedding in outcrop.

4.1.6. Calcareous siltstone (CSt)

The calcareous siltstone facies (CSt) is composed primarily brown to pinkish beds of silt-sized siliciclastic grains with a variable amount of carbonate matrix and cement. Petrographic analysis shows that grains are dominantly silt-sized with minor very fine, subrounded–subangular sand grains (Fig. 7H, I). Quartz grains are the most common mineralogy with minor amounts of chert lithic grains and lithic grains composed of fine groundmass. Opaque oxide grains are present and often well-distributed in thin sections, likely contributing to the brown to pink color in hand sample. Opaque, likely organic-rich, matrix material between grains is also common. Mineral composition by X-ray diffraction includes quartz, calcite, plagioclase feldspar, and illite-group minerals (Fig. 5). No body fossils were observed in this facies from this work; however, they have been previously reported (Ward et al., 2007; Taylor et al., 2021). Both in the thin section and outcrop, facies CSt is commonly planar and cross-laminated. The tops of beds are commonly mottled, indicating bioturbation, and planar dense cf. *Palaeophycus* can be found on some bedding planes. Bedding is typically thin to medium (typically 5–20 cm), but bedding planes in the calcareous siltstone facies can be difficult to differentiate, giving the appearance of thick to massive bedding (>50 cm). Facies CSt gradationally overlies facies SLMW and is commonly found interbedded with facies SLMW (Fig. 6C–E).

4.2. Stratigraphy of the Gabbs Formation

The general stratigraphy of the Gabbs Formation is consistent across its exposure range in the New York Canyon area. The lower 36–55 m of

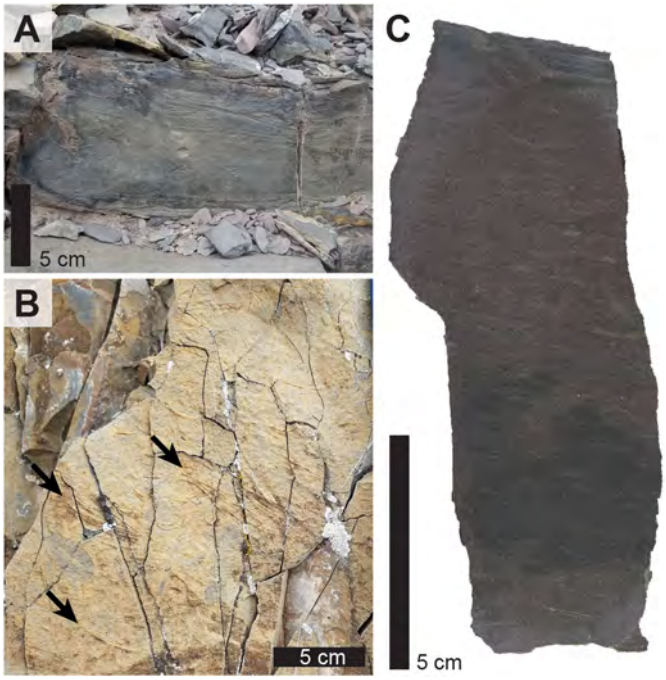

Fig. 8. Sedimentary structures from Gabbs Formation facies. (A) Wavy to trough lamination common in purple lime mudstone facies. (B) Interrupted cross-lamination highlighted by differential erosion found in silty lime mudstone–wackestone facies. (C) Trough-cross lamination in calcareous siltstone facies.

the unit (Nun Mine Member) is composed of interbedded calcareous siltstone (CS) and purple lime mudstone (PLM) facies (Fig. 4). Individual beds are traceable over short distances within single exposures (Fig. 6A); however, in weathered sections, such as the measured section 6, along New York Canyon Road, individual beds of PLM are obscured and more difficult to distinguish from CS facies. Up-section beds of facies PLM become more frequent and rare fossiliferous beds of facies SPF are also interbedded. The transition from the lower interbedded CS and PLM facies to the more resistant beds of facies SPF is rapid but appears conformable.

The middle approximately 70 m of the Gabbs Formation (Mount Hyatt Member) is dominated by carbonate beds of facies skeletal packstone–floatstone (SPF) and hashy skeletal packstone (HSP) for the first 35 m and by facies silty lime mudstone–wackestone (SLMW) for the next 20–35 m. Most beds in the lower portion of the middle unit are skeletal packstone with occasional larger fossils and are interbedded with common beds of more fossiliferous floatstone beds. Up-section occasional beds of HSP become interbedded with facies SPF. Above where beds of facies HSP are found, beds of facies SPF become interbedded with facies SLMW and facies SLMW dominates up-section. The frequency of fossiliferous SLMW beds is variable across the exposure area. Where facies SLMW is dominant, it becomes increasingly silty and interbedded with thin beds of facies calcareous siltstone (CSt) up-section. Interbedding of facies SLMW and CSt begins up to 15 m below where facies SLMW is lost. The upper part of the middle carbonate unit (upper Mount Hyatt Member) records a gradual decline of carbonate and an increasing amount of siliciclastic material.

The uppermost approximately 15 m of the Gabbs Formation (Muller Canyon Member) is dominated by facies CSt. The amount of interbedding with facies SLMW is variable among columns (Fig. 4; measured sections 2, 7–8) and may reflect the position of these measured sections relative to the shoreline. Bedding is difficult to distinguish in facies CSt owing to extensive weathering, but more cohesive bed samples tend to fine up-section from coarse silt and fine sand to fine silt. Near the top of the Gabbs Formation, several lime mudstone beds consistent with facies of the Sunrise Formation and containing Jurassic-age fossils, interbed with facies CSt. (Hallam and Wignall, 2000; Ritterbush et al., 2014). Ritterbush et al. (2014) noted that the lowest of these beds were silty, supporting the observation of a gradational upper contact of the Gabbs Formation and the Sunrise Formation.

5. Discussion

5.1. Facies interpretation

Facies CS (calcareous shale) is interpreted to represent deposition in the outer ramp. The high carbonate and siliciclastic mud content indicates that this environment is lower energy and therefore likely more basinward of deposits with larger grain size (Read, 1985; Burchette and Wright, 1992).

Facies PLM (purple lime mudstone) is interpreted to represent higher energy deposition events, such as storms, in an outer ramp setting. Facies PLM remains fine-grained, indicating a lower energy environment than mid-ramp settings that would experience more reworking (Read, 1985; Burchette and Wright, 1992). The presence of primarily ammonite fauna with rare benthic taxa supports a deep ramp setting (Laws, 1982). Common wavy laminations in carbonate PLM beds containing fossils are indicative of storm beds, and their thin bedding with abundant interbeds of facies CS, places many beds of PLM as distal storm beds (Aigner, 1985; Tucker and Wright, 1990; James and Dalrymple, 2010). Visible siliciclastic grains are extremely rare in facies PLM indicating little terrigenous material not in suspension is transported to the outer ramp environment.

Facies SPF (skeletal packstone–floatstone) is interpreted to represent deposition in a mid-ramp setting. The increased grain size in the carbonate matrix of these lithologies as well as the common to abundant large and diverse skeletal clasts and low carbonate mud content indicate frequent reworking in a moderate energy shallow-subtidal environment on the mid-ramp between fair-weather and storm wave base (Burchette and Wright, 1992; James and Dalrymple, 2010; Read, 1985; Tucker and Wright, 1990). Wavy bedding planes found in these deposits may indicate storm influence though no hummocky cross stratification was found in these deposits (Aigner, 1985; Tucker and Wright, 1990).

Facies HSP (hashy skeletal packstone) is interpreted to represent deposition of bioclastic shoals on the mid to inner ramp transition. Facies HSP corresponds to a high energy setting owing to its abundance of fragmentary mollusks and echinoderm skeletal grains as well as its fine sand matrix of biogenic grains (Read, 1985; Burchette and Wright, 1992; James and Dalrymple, 2010). The gradational lower contacts of facies HSP with facies SPF indicate it is a higher energy-adjacent mid-ramp environment; however, the fact that facies SPF is also found interbedded with facies SLMW, without facies HSP, indicates the higher-energy accumulation of skeletal grains found in facies HSP is likely a laterally discontinuous shoal positioned near the inner ramp transition. Facies HSP also commonly contains fine angular to subangular quartz grains indicating a more proximal position to the source of terrigenous material than facies SPF, PLM, or CS.

Facies SLMW (silty lime mudstone–wackestone) is interpreted to represent deposition in an inner ramp transition setting. The carbonate mudstones with abundant and visible siliciclastic very fine sand to silt grains indicate that facies SLMW is likely closer to the terrigenous source than facies HSP. The decrease in overall grain size is likely due to a slight increase in water depth landward of the discontinuous bioclastic shoal, facies HSP. Facies SLMW's position in the inner ramp transition is also indicated by its interbedding with both facies SPF and CSt, which likely places facies SLMW between facies SPF and CSt on the inner ramp transition.

Facies CSt (calcareous siltstone) is interpreted to represent deposition on the distal inner ramp in a lower intertidal portion of a tidal flat. The silt–very find sand grains composing at least 50% of facies CSt,

are primarily quartz but also include more easily weathered lithic fragments and plagioclase feldspars were also detected in X-ray diffraction. The mineralogy along with the abundant cross laminae and bioturbation, indicates a shallow marine environment in close proximity to a terrigenous sediment source (James and Dalrymple, 2010). A shallow interpretation is supported by the lack of open marine pelagic fossils expected in return to deeper outer ramp environments. Tidal influence is indicated by the common alternating tabular cross and planar lamination in beds which can be indicative of tidal flats with strong wave influence where the drop in energy during slack tide is not low enough to allow muds to settle from suspension (Yang et al., 2005). The decrease in grain size up-section within this facies is also consistent with a tidal flat interpretation (Flemming, 2003; Dalrymple and Choi, 2007). In carbonate systems that shallow into fine siliciclastic sediments, the source of the fine material is thought to be originally transported to the shelf from floods and then transported away from the fluvial delta by longshore currents (Coffey and Read, 2004). This scenario appears likely in the case of facies CSt as the grain sizes are small and easily transported and still carry a proximal terrigenous signal (lithics and feldspars), but sediments from the source delta itself are not preserved in the Gabbs Formation.

5.2. Facies association

Facies relationships in the southern Gabbs Valley Range indicate the Gabbs Formation was deposited on the outer to distal inner ramp portions of a mixed carbonate-siliciclastic ramp (Fig. 9). The gradual vertical transitions between facies, indicated by gradational contacts and intertonguing between facies, demonstrate the lateral adjacency of their original depositional environments.

The repeated appearance of facies relationships in multiple measured sections allows for the reconstruction of this ramp environment. Facies CS (calcareous shale) represents the most basinward environment and is interpreted to have been deposited on the outer ramp. Facies CS is interbedded with facies PLM (purple lime mudstone), with facies PLM gradually dominating in lithology up-section. Facies PLM is interpreted to represent slightly more proximal outer ramp storm deposits. Facies PLM is overlain sharply, but conformably, and interbeds slightly with facies SPW (skeletal packstone–floatstone). The increase in grain size from facies PLM to SPF is interpreted to represent an increase in energy in the more landward mid-ramp setting of facies SPF. Facies SPF occasionally grades vertically into facies HSP (hashy skeletal packstone) interpreted to represent a discontinuous shoaling environment along the proximal mid-ramp. Where facies HSP is absent, facies SPF interbeds with facies SLMW (silty lime mudstone–wackestone), where the carbonate mud and quartz silt rich beds of facies SLMW gradually come to lithologically dominate. Up-section, facies SLMW interbeds with facies CSt (calcareous siltstone) and facies CSt gradually becomes lithologically dominant. This relationship places facies SLMW in the inner ramp transition. Facies CSt is interpreted to represent deposition on the distal inner ramp to a deep subaqueous portion of a tidal flat indicated by the dominance of terrigenous grains in the lithology of the facies. Overall, the Gabbs Formation represents deposition on a carbonate outer to mid-ramp transitioning to a siliciclastic-dominated inner ramp.

This facies association agrees well with previous work considering the entirety of the Gabbs Formation (Laws, 1978, 1982; Taylor et al., 1983). Previous work has also described the Gabbs Formation depositional setting as a carbonate ramp with proximal terrigenous input (Laws, 1978, 1982), though did not arrange these facies into a depositional model. The model proposed in this work includes all previously described lithologies that were able to be confirmed using multiple stratigraphic sections.

Laws (1978) identified a facies that this work was unable to confirm using multiple correlative stratigraphic sections. This author interpreted a thin interval of spherical grains, described therein as pisolites composed of calcite and terrigenous clay, in sparry calcite approximately where facies PLM begins to interbed with facies SPF; Laws (1978) placed them in a more landward environment than our facies model suggests based on adjacent facies. However, the presence of pisolites is inconsistent with the interpretation of outer to mid-ramp environments for facies PLM and SPF. This study only identified a small outcropping of these pisolites at supplementary site 12 and was unable to verify their consistent presence or exact stratigraphic location in other measured sections during the course of mapping. If the stratigraphic location of the interpreted pisolites can be confirmed at the boundary between facies PLM and SPF in subsequent fieldwork, the deposit may be better characterized as a feature of a sequence boundary, rather than a facies, given its abrupt appearance in otherwise mid to outer ramp deposits. For these reasons, the pisolite deposit was not considered as an

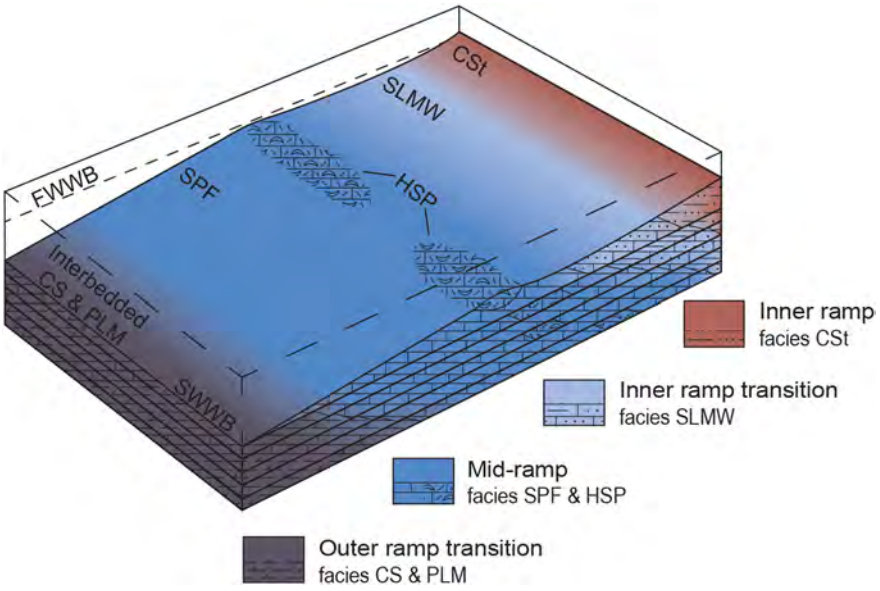

Fig. 9. Gabbs Formation facies model. Three-dimensional representation of the spatial association of facies in the Gabbs Formation. Facies represent deposition on a carbonate ramp with landward terrigenous sedimentation.

environment in the overall facies association. Further work that establishes the exact nature and position of this deposit may subsequently alter this proposed facies association.

5.3. Sequence stratigraphic interpretations of the Gabbs Formation

The stratigraphic architecture within the Gabbs Formation records a primarily regressive depositional interval on a mixed carbonate-siliciclastic ramp (Figs. 4, 9) ending in a transgressive interval in the uppermost approximately 5 m of the Gabbs Formation, near the contact with the overlying Sunrise Formation. The lowest portion of the Gabbs Formation represents a significant deepening from the shallow dolostones of the underlying Luning Formation. The boundary itself is sharp, but there is no evidence of subaerial exposure or erosion, though the Luning–Gabbs formation boundary is altered in many areas as the upper Luning Formation is commonly a host for hydrothermal deposits in the Gabbs Valley Range (Silberling and Jones, 1984). This common alteration may obscure the original nature of the Luning–Gabbs formation boundary. Above the boundary are interbedded facies PLM and CS beds of the outer ramp transition deposits. The Luning–Gabbs Formation boundary likely represents a transgressive surface or drowning unconformity where the increase in water depth was sufficient to halt the shallow water dolostone deposition, though not enough to entirely halt carbonate deposition for a significant time. Individual parasequences are difficult to distinguish within interbedded outer ramp facies CS and PLM, but the overall consistency of the interbedding for most of lower measured sections implies aggradational stacking for most of their exposure and stacking becomes increasingly progradational up-section as facies PLM becomes the dominant lithology, displaying a keep-up style of carbonate deposition (Tucker et al., 1993).

The transition to progradational stacking is apparent with the appearance of the skeletal packstone–floatstone (SPF) facies of the mid-ramp deposits (Fig. 4). Parasequences rapidly gain facies SPF at the top and lose the distinctly purple-colored facies PLM and CS from the bottom. The transition between parasequences dominated by outer ramp transition facies and parasequences dominated by mid-ramp facies is rapid, usually happening within only a few meters, and begins a clear progradational stacking pattern up-section within the mid-ramp facies. Rare beds of facies SPF appear lower in the New York Canyon Road measured section (Fig. 4; measured section 6), providing additional evidence of more easterly outcrops being positioned more landward, as these shallower facies should appear in more landward sections stratigraphically lower than more basinward sections. The uppermost beds of facies PLM at supplementary site 12 (Fig. 3) contain a thin deposit of large spherical carbonate-containing grains. These grains have been previously interpreted as pisolites and imply a much shallower high energy environment (Laws, 1978) and a forced regression. As discussed in the facies association, this feature was not found in multiple sections and was therefore excluded from the interpretation.

Progradational stacking patterns continue with the addition of inner ramp transition and inner ramp facies. Facies HSP appears at the top of parasequences more frequently up-section (Fig. 4), followed by the appearance of facies SLMW containing more terrigenous silt. The appearance and frequency of facies HSP are variable among columns containing mid-ramp deposits, indicating that facies HSP was likely not a laterally extensive parallel to strike facies belt, but discontinuous distribution of local shoals. The interbedding of facies SPF and SLM in the Mine Test, Combo Canyon, and Muller Canyon sections (Fig. 4) supports this interpretation. Facies SLMW tends to become siltier up-section and interbeds with inner ramp facies CSt.

In measured sections Mine Test and Combo Canyon (Fig. 4), the frequency of interbedded carbonate facies SLMW decreases up-section as terrigenous facies CSt increases, until the carbonate facies is lost entirely. The gradual loss of carbonate facies is similar in manner as other more basinward facies, indicating that it is a predictable change from a carbonate to siliciclastic-dominated environment as the system shallows from shallow-subtidal mid-ramp to tidally influenced environments. In many studies of the Muller Canyon section and Triassic–Jurassic boundary, the loss of carbonate facies SLMW is pictured as very abrupt (Guex et al., 2004; Lucas et al., 2007; Ward et al., 2007; Hallam and Wignall, 2000; Thibodeau et al., 2016); however, an analysis of additional correlative sections demonstrates that this is not the typical case; in fact, facies CSt is found interbedded with facies SLMW as much as 15 m below the loss of facies SLMW (Figs. 4, 6).

The gradational and primarily shallowing-upwards trend of most of the Gabbs Formation facies indicates a period of normal regression best interpreted as a potential highstand system tract. The progradational stacking of parasequences as evidenced by the appearance of increasingly landward facies and loss (without a return) of more basinal outer ramp transition facies up-section supports this interpretation. The point of turnaround from progradational to retrogradational stacking seen in the uppermost part of the Gabbs Formation and near the Gabbs–Sunrise Formation boundary is also difficult to distinguish within the calcareous siltstone facies. The reappearance of mid-shelf carbonates around the Gabbs–Sunrise boundary and in the lower Sunrise Formation (Ritterbush et al., 2014, 2016) indicates backstepping and necessitates a transgressive surface or correlative surface in the uppermost Gabbs Formation.

In the uppermost 6 m of the Gabbs Formation there is a return of carbonate beds. These carbonates, containing Jurassic-age fossils including *Psiloceras* (Muller and Ferguson, 1936, 1939; Guex et al., 2004; Ward et al., 2007; Thibodeau et al., 2016; Taylor and Guex, 2021), are more similar in composition to the mid-ramp deposits of the overlying Sunrise Formation than carbonates found lower in the Gabbs Formation (Ritterbush et al., 2014, 2016; Clement et al., 2020). This similarity of carbonate facies supports a deepening of the system back to mid-ramp environments immediately below the formational boundary with the Sunrise Formation, which is placed at the first carbonate bed of medium thickness (Taylor et al., 1983). The backstepping pattern is best seen in the Muller Canyon measured section, as the siltstones outcrop poorly at Mine Test, and the siltstones are directly juxtaposed with overlying bedded chert by a fault at Combo Canyon (Fig. 6E, F).

General basin characteristics can still be interpreted from the Gabbs Formation, despite structural complexities present in the Gabbs Valley Range and limited exposure of the Gabbs Formation in other locations, complicating the basin-wide interpretation. In the vicinity of New York Canyon, the Gabbs Formation outcrops repeatedly on at least four thrust sheets with the original orientation of the measured sections within the cross section (Fig. 4) being northwest–southeast. This original line was likely oriented oblique to strike owing to the similarity of facies stacking patterns and general thicknesses of each depositional environment but a variation in facies expression among columns. Additionally, no evidence of significant distal steepening or platform margin build-ups is present in the Gabbs Formation from the Gabbs Valley Range, indicating the portion of the southeastern margin of the back-arc basin preserved in the Gabbs Formation was most likely ramp-like in its geometry. The results and interpretations of this work agree well with most previous interpretations (Laws, 1978, 1982; Taylor et al., 1983) as well as the general basin geometry interpretations made from the underlying Luning Formation (Speed, 1978; Reilly et al., 1980; Oldow, 1984).

5.4. Comparison of stratigraphic architecture to previous work

Previous work has only addressed the stratigraphic architecture of the Gabbs Formation tangentially or within specific members, leading to misinterpretations of the members based on previous descriptions. In-depth descriptions of the members are provided in Supplemental materials to accompany the facies descriptions and facilitate clarity for future research at this significant site. The general shallowing-upward regressional nature of most of the Gabbs Formation is recognized by Laws (1978, 1982) and Taylor et al. (1983) as well as the upper

transgression marked by the reappearance of carbonates near the Gabbs–Sunrise formational boundary. Most previous works focused primarily on the Triassic–Jurassic boundary have also noted the increased terrigenous input, decrease in grain size, ripples, and increased bioturbation indicative of shallowing in the upper Mount Hyatt and Muller Canyon Members and the deepening to carbonates at the very top of the Muller Canyon Member (Guex et al., 2004; Hallam and Wignall, 2000). Implications of transgressions at the lower boundary with the Luning Formation are not discussed.

The present research supports previous interpretations of general shallowing-upwards in the Gabbs Formation and addresses the architecture of the Gabbs Formation as a whole. This work also recognizes the shallowing into mid-ramp environments in the Nun Mine and Mount Hyatt Members as well as the increased terrigenous input, decreased grain size, ripples, and increased bioturbation noted by previous authors as evidence of shallowing in the Mount Hyatt and Muller Canyon Members. Likewise, this work recognizes deepening in the uppermost Muller Canyon Member. The necessary deepening from the Luning Formation to the Nun Mine Member is also addressed. This work adds an in-depth analysis of facies and stacking patterns which support and add more details to a basic sequence stratigraphic framework of previous interpretations.

A deepening has been postulated for the Mount Hyatt Member–Muller Canyon Member transition by other workers; however, our observations do not support this interpretation. A deepening between the upper Mount Hyatt Member and lower Muller Canyon Member was posited by Lucas et al. (2007), based on features such as ripples (as storm features), horizontal bioturbation (*Helminthoides*, part of the *Nereites* ichnoassemblage), and presence of radiolarians. However, no evidence was found to confirm the presence of turbidite deposits that would be part of the storm-feature ripples' presentation, nor was evidence observed for systematic bedding-plane traces that would be consistent with a *Nereites* interpretation. Further, Orchard et al. (2007) only report a single sample with one radiolarian genus from the calcareous siltstone facies in the Muller Canyon Member. The increasing terrigenous input along with ripple laminations and bioturbation levels found in facies CSt, which are all dissimilar from deep-water facies found in the Gabbs Formation, supports a more landward interpretation for the siltstone deposits in the Muller Canyon Member.

5.5. Global stratigraphic architecture of Late Triassic and Triassic–Jurassic boundary sections

The sedimentary record of the Gabbs Formation is critical for interpreting the biological, sedimentological, geochemical, and sequence stratigraphic aspects of the latest Triassic, regionally and globally. The Gabbs Formation represents one of few shallow-marine Panthalassan examples of the Late Triassic and the only Panthalassan locality where the Rhaetian marine regression appears normal rather than forced as it appears in shallow-marine deposits in Sonora, Mexico and British Columbia, Canada (Williston Lake). By comparing multiple sections across the exposure area of the Gabbs Formation, the transition from mid-ramp packstone beds to inner ramp transition silty lime mudstone beds and finally to inner ramp calcareous siltstones was found to be gradual and did not display any evidence of an abrupt shallowing (i.e. surface of forced regression) nor subaerial exposure or hiatus.

Other Norian–Early Jurassic Panthalassan sections exhibit characteristics of forced regression. In contrast to the nearly continuous depositional record of the New York Canyon locality, Wignall et al. (2007) found a significant depositional hiatus, spanning most of the Rhaetian, in the most proximal exposures in the Pardonet and Fernie formations of Williston Lake, British Columbia. In distal sections from the same formations, sedimentation can be continuous but is marked by unique facies such as a Rhaetian shallow-marine phosphatic ooid lowstand deposit (Wignall et al., 2007; Larina et al., 2019). Sedimentary units from Sonora, Mexico show an abrupt shallowing in the Norian–Rhaetian Antimonio Formation during an interval otherwise interpreted as a transgression. The Rhaetian deposits are notably thin and are primarily a lag deposit of shallow-marine fossils and eroded coral build-up clasts showing vadose weathering, possibly indicating a forced regression (González-León et al., 1996). The deep-water Kennecott Point, British Columbia exposure has a similar architecture to those in Sonora and Williston Lake. Wignall et al. (2007), based on Ward et al. (2004), posit that a package of thick-bedded sandstone turbidite beds, in otherwise more distal silts and shales, represents a lowstand deposit immediately prior to the initial negative carbon isotope excursion (ICIE) near the end of the Rhaetian and a return to deeper conditions. Shallowing prior to the ICIE is also seen in the normal regression in Nevada (Guex et al., 2004; Ward et al., 2007; Guex et al., 2009; Thibodeau et al., 2016); however, the Gabbs Formation's continuous deposition records shallow-marine environments important for the study of the end-Triassic mass extinction. The continuous shallow-marine deposition of the Gabbs Formation stands out among other Late Triassic Panthalassan deposits where forced regression produced a hiatus and/or the deposition of unique lowstand facies.

The depositional record in the Gabbs Formation may have implications for the Tethyan marine realm where deposition in the Rhaetian Stage is often characterized by many higherorder transgressive–regressive cycles (Gianolla et al., 1998; Haas and Tardy-Filácz, 2004; Hesselbo et al., 2004; Rožič et al., 2009; Ruhl et al., 2009; Haas et al., 2010). In places such as Csővaŕ, Hungary and St. Audrie's Bay, United Kingdom, higher order cycles show evidence of abrupt shallowing in the late Rhaetian (Haas and Tardy-Filácz, 2004; Hesselbo et al., 2004; Haas et al., 2010). Other localities, such as the Slovenian Basin in the eastern Southern Alps and the Kössen and Kendlbach formations in Austria, show less abrupt shallowing of relative sea-level, or normal regression, in the late Rhaetian followed by a transgression through the Triassic–Jurassic boundary similar to sedimentation in the Gabbs Formation (Rožič et al., 2009; Ruhl et al., 2009). However, records from many central European basins, including most of the Southern Alps, the Northern Calcareous Alps, the Paris Basin, and the German Basin, characterize the entirety of the Rhaetian as a first or second order transgression, with higher order sequences occurring more locally (Gianolla and Jaquin, 1998; Goggin and Jaquin, 1998; Aigner and Bachman, 1998). Similar to the Gabbs Formation, these differences in relative sea-level likely reflect regional tectonic effects in the complex sedimentary basins of the Tethyan realm.

The regression recorded in the Gabbs Formation is characterized across its exposure area as a gradual shallowing upwards indicating a pattern of normal regression during most of the Rhaetian in Nevada. The comparison of multiple sections from outside the well-studied section at Muller Canyon supports this interpretation and suggests a better depositional record without extensive hiatuses. There is also no evidence of subaerial exposure or erosion prior to the onset of deepening at the Triassic–Jurassic Boundary in Nevada. This nearly continuous deposition in New York Canyon may be due to local tectonic effects overprinting the global, potential eustatic, drop in sea level, resulting in the Gabbs Formation recording a normal regression where relative sea-level is still rising, but at a reduced rate (i.e. a highstand systems tract). The shallow-marine deposition recorded in the Gabbs Formation makes it an ideal candidate to compare a continuous section from Panthalassa to those from Tethys.

5.6. Carbonate decline, the timing of acidification, and the Triassic–Jurassic boundary in New York Canyon

The Triassic–Jurassic boundary, globally and in the Gabbs Formation, is associated with a carbonate crisis and global ocean acidification event (Hautmann et al., 2008; Schaltegger et al., 2008; Greene et al., 2012; Martindale et al., 2012; Ikeda et al., 2015). Evidence from the Gabbs Formation includes carbon and mercury isotopic excursions (Guex et al.,

2004; Ward et al., 2007; Thibodeau et al., 2016). These excursions, considered to be associated with acidification and the end-Triassic mass extinction (Schaltegger et al., 2008; Schoene et al., 2010), have only been analyzed from measured section 8 (Muller Canyon) (Fig. 7) where the gradual loss of carbonate facies is present below the excursions but is rarely studied or pictured in its entirety (Guex et al., 2004; Ward et al., 2007; Thibodeau et al., 2016; Larina et al., 2021). The loss of carbonate facies SLMW in the Muller Canyon section also superficially appears abrupt due to an intrusive aplite sill approximately 10 m below the excursions obscuring the gradual nature of the carbonate decline (Fig. 6E). This has led to the interpretation of the Gabbs Formation as containing a potential carbonate hiatus related to the onset of acidification (Greene et al., 2012). While the final loss of carbonate facies SLMW does occur in close stratigraphic proximity to the initial negative carbon isotope excursion (ICIE), approximately 1 m below, lower portions of the Muller Canyon measured section show facies SLMW and CSt begin interbedding 6 m below the aplite sill intrusion. The facies transition is better exposed in outcrop and occurs even more gradually in the Mine Test and Combo Canyon measured sections (Fig. 4; measured sections 2, 7) indicating that the decline of carbonate facies SLMW began before the ICIE and onset of acidification.

A recent study by Larina et al. (2021) analyzed the carbon and mercury isotopic records and fossils for 7 m below the ICIE in Muller Canyon. Their findings suggest a precursor carbon isotope excursion approximately 5.5 m below the ICIE and low diversity benthic fossil assemblages (Larina et al., 2021). This suggests low oxygen or acidifying conditions may appear earlier than previously realized; however, the transition between facies SLMW and CSt begins well below this study interval and continues until just below the ICIE. Even with a potential early onset of acidification, an increase in terrigenous material and decline of carbonate was already in progress.

The baseline sedimentation change, from dominantly carbonate to siliciclastic, may have aided in the deposition and preservation of more Late Triassic sediments in the Gabbs Valley Range than elsewhere in Panthalassa. The upper Gabbs Formation does not show any evidence of a protracted depositional hiatus resulting from a forced regression or potentially from acidifying conditions in a carbonate environment. In other sections in Panthalassa and Tethys, erosion or depositional hiatuses mean the extinction interval, isotopic excursions, and Triassic–Jurassic boundary occur nearly simultaneously or have positions that are difficult to interpret (Hesselbo et al., 2004; Wignall et al., 2007; Hautmann et al., 2008). The more continuous deposition of the Gabbs Formation and slow transition to terrigenous sediment allow for these events to be identified individually.

The initial increase in terrigenous material begins with the introduction of facies SLMW, up to 35 m below the ICIE. The decline of carbonate facies and transition to shallow terrigenous facies continue the gradual interbedding of facies SLMW and CSt up section, approximately 20–1 m below the ICIE (Fig. 4; measured section 8). Acidifying conditions may have begun during this transition interval (Larina et al., 2021), but the ICIE marking the extinction interval and onset of acidification (often recognized by a carbonate dissolution or hiatus) does not occur until 1 m above the last medium bed of facies SLMW. Carbonate loss from the acidification is more likely recorded as the reduction in carbonate content in facies CSt up-section reported by Guex et al. (2004). The primarily siliciclastic facies CSt records excursion-level δ^{13}Corg values for approximately 4 m above the ICIE (Guex et al., 2004; Ward et al., 2007; Guex et al., 2009; Thibodeau et al., 2016), a larger stratigraphic interval than other Triassic–Jurassic boundary sections found globally (Korte et al., 2018). The protracted isotope excursion and the lack of fossils found in this study in facies CSt between the ICIE and the lower beds of the overlying Sunrise Formation (14 m interval) potentially provide evidence for the duration of the acidification, preserved without hiatus. Though others have found fossils in this interval, most notably *Psiloceras spelae* which marks the beginning of the Jurassic (Guex et al., 2004; Ward et al., 2007), fossils are still exceedingly rare supporting a continuation of acidifying conditions up to the Triassic–Jurassic boundary. The boundary itself, located approximately 8 m above the ICIE, and the slow return of fossils to the system, may signal the end of acidifying conditions and are accompanied by deepening back into the carbonate mid-ramp setting of the Sunrise Formation (Ritterbush et al., 2014). However, unique facies of the Sunrise Formation indicated a more protracted period of geochemical perturbations (Ritterbush et al., 2014; Ritterbush et al., 2016; Clement et al., 2020). With the continuous, primarily siliciclastic, deposition in the uppermost Gabbs Formation, it is possible to consider the background sedimentation decline of carbonate facies, the acidification and extinction intervals, and the position of the Triassic–Jurassic boundary individually.

6. Conclusions

The Gabbs Formation represents a period of transgressive–regressive–transgressive deposition on a mixed carbonate-siliciclastic ramp with outer ramp transition to inner ramp environments. The lower Nun Mine Member represents the first transgression of outer ramp transition facies over the shallow dolostones of the underlying Luning Formation. The progradational stacking patterns and shallowing of facies to inner ramp environments in the upper Nun Mine Member, through the Mount Hyatt Member, and into the lower Muller Canyon Member represent a normal regression from carbonates into terrigenous siltstones. The final transgression straddles the formational boundary between the Gabbs and overlying Sunrise, indicated by the appearance of mid-ramp carbonate facies, in the primarily inner ramp calcareous siltstones of the Muller Canyon Member, which are similar to those found higher in the Ferguson Hill Member. The lack of subaerial exposure makes some significant stratigraphic surfaces difficult to identify. Potential surfaces, and intervals of shallowing and deepening, are indicated by changes in stacking patterns of facies.

In-depth analysis of facies succession in the Gabbs Formation supports the interpretation that the decline of carbonate-dominated facies in the upper Gabbs formation, between the Mount Hyatt Member and the Muller Canyon Member, is not a result of acidification processes associated with the End-Triassic mass extinction. Rather, evidence of acidification is best observed within the Muller Canyon Member siltstones, recognized by carbon isotope excursions, disappearance of various calcareous marine invertebrates, and unusual carbonate facies in the overlying Sunrise Formation.

By establishing the primary decline of carbonate facies as baseline sedimentation that begins well below the isotopic excursions, acidification and extinction intervals, and Triassic–Jurassic boundary recorded in the calcareous siltstone facies, each of these features, and their relative timing, can be considered individually with minimal concern of a hiatus due to acidifying conditions in a primarily carbonate environment. This makes the Gabbs Formation an ideal section for global comparisons of Late Triassic continuous sections.

Supplementary data to this article can be found online at https://doi.org/10.1016/j.sedgeo.2021.106021.

Declaration of competing interest

The authors declare that they have no known competing financial interests or personal relationships that could have appeared to influence the work reported in this paper.

Acknowledgements

This research was conducted on the traditional lands of the Northern Paiute and their ancestors. American settlers and the Government of the United States forcibly removed the Northern Paiute people from much of their homeland, including the area of this research, in the mid 1800's. Their descendants are part of the Walker River Paiute Tribe and many reside on the Walker River Paiute Indian Reservation.

This research was supported by the National Science Foundation (NSF) [CAREER Award #1654008], the Geological Society of America [Graduate Student Research Grant], and the Association of Applied Paleontological Sciences [James R. Welch Scholarship]. The authors would like to thank Kaitlyn Fleming, Sara Gibbs-Schnucker, and Haley Marsten for assistance in the field, Dr. Kathleen Ritterbush and Dr. Yadira Ibarra for additional field photographs, and UC Berkeley Libraries. The authors also thank Dr. David Hopkins and Rodney Utter from NDSU Dept. of Soil Science for the use of thin section equipment, and the NDSU Materials Characterization and Analysis Laboratory for assistance with X-ray diffraction.

References

Aigner, T., 1985. Storm depositional systems. In: Friedmann, G.F., Neugebauer, H.J., Seilacher, A. (Eds.), Lecture Notes in Earth Sciences. vol. 3. Springer-Verlag, Berlin, Germany (174 pp.).

Aigner, T., Bachman, G.H., 1998. Triassic sequence stratigraphy in the intra-cratonic German basin (summary of published paper). In: de Graciansky, P.C., Hardenbol, J., Jaquin, T., Vail, P.R. (Eds.), Mesozoic and Cenozoic Sequence Stratigraphy of European Basins. SEPM Special Publicationsvol. 60, pp. 749–751.

Burchette, T.P., Wright, V., 1992. Carbonate ramp depositional systems. Sedimentary Geology 79, 3–57.

Clement, A.M., Tackett, L.S., Ritterbush, K.A., Ibarra, Y., 2020. Formation and stratigraphic facies distribution of early Jurassic iron oolite deposits from west central Nevada, USA. Sedimentary Geology 395, 105537. https://doi.org/10.1016/j.sedgeo.2019.105537.

Coffey, B.P., Read, J., 2004. Mixed carbonate–siliciclastic sequence stratigraphy of a Paleogene transition zone continental shelf, southeastern USA. Sedimentary Geology 166, 21–57.

Dalrymple, R.W., Choi, K., 2007. Morphologic and facies trends through the fluvial-marine transition in tide-dominated depositional systems: a schematic framework for environmental and sequence-stratigraphic interpretation. Earth-Science Reviews 81, 135–174.

Dunham, R.J., 1962. Classification of carbonate rocks according to depositional textures. AAPG Memoir 1, 108–121.

Embry, A.F., Klovan, J.E., 1971. A late Devonian reef tract on northeastern Banks Island, N.W.T. Bulletin of Canadian Petroleum Geology 19, 730–781.

Ferguson, H.G., Muller, S.W., 1949. Structural geology of the Hawthorne and Tonopah quadrangles, Nevada. Geological Survey Professional Paper 216. US Government Printing Office, Washington D.C.

Flemming, B.W., 2003. Tidal flats. In: Middleton, G.V., Church, M.J., Coniglio, M., Hardie, L.A., Longstaffe, F.J. (Eds.), Encyclopedia of Sediments and Sedimentary Rocks. Kluwer Academic Publishers, Dordrecht, Netherlands, pp. 734–737.

Gianolla, P., Jaquin, T., 1998. Triassic sequence stratigraphic framework of western European basins. In: de Graciansky, P.C., Hardenbol, J., Jaquin, T., Vail, P.R. (Eds.), Mesozoic and Cenozoic Sequence Stratigraphy of European Basins. SEPM Special Publicationsvol. 60, pp. 643–650.

Gianolla, P., de Zanche, V., Mietto, P., 1998. Triassic sequence stratigraphy in the Triassic system of the western Southern Alps. In: de Graciansky, P.C., Hardenbol, J., Jaquin, T., Vail, P.R. (Eds.), Mesozoic and Cenozoic Sequence Stratigraphy of European Basins. SEPM Special Publicationsvol. 60, pp. 719–748.

Goggin, V., Jaquin, T., 1998. A sequence stratigraphic framework of the marine and continental Triassic series in the Paris basin, France. In: de Graciansky, P.C., Hardenbol, J., Jaquin, T., Vail, P.R. (Eds.), Mesozoic and Cenozoic Sequence Stratigraphy of European Basins. SEPM Special Publicationsvol. 60, pp. 667–690.

González-León, C.M., Taylor, D.G., Stanley, G.D., 1996. The Antimonio Formation in Sonora, Mexico, and the Triassic-Jurassic boundary. Canadian Journal of Earth Sciences 33, 418–428.

Greene, S.E., Martindale, R.C., Ritterbush, K.A., Bottjer, D.J., Corsetti, F.A., Berelson, W.M., 2012. Recognising ocean acidification in deep time: an evaluation of the evidence for acidification across the Triassic–Jurassic boundary. Earth-Science Reviews 113, 72–93.

Guex, J., Bartolini, A., Atudorei, V., Taylor, D.G., 2004. High-resolution ammonite and carbon isotope stratigraphy across the Triassic–Jurassic boundary at New York Canyon (Nevada). Earth and Planetary Science Letters 225, 29–41.

Guex, J., Bartolini, A., Taylor, D.G., Atudorei, V., Thelin, P., Bruchez, S., Tanner, L.H., Lucas, S.G., 2009. Comment on: "The organic carbon isotopic and paleontological record across the Triassic–Jurassic boundary at the candidate GSSP section at Ferguson Hill, Muller Canyon, Nevada, USA" by Ward et al. (2007). Palaeogeography, Palaeoclimatology, Palaeoecology 273, 200–204.

Haas, J., Tardy-Filácz, E., 2004. Facies changes in the Triassic–Jurassic boundary interval in an intraplatform basin succession at Csővár (Transdanubian Range, Hungary). Sedimentary Geology 168, 19–48.

Haas, J., Götz, A.E., Pálfy, J., 2010. Late Triassic to early Jurassic palaeogeography and eustatic history in the NW Tethyan realm: new insights from sedimentary and organic facies of the Csővár Basin (Hungary). Palaeogeography, Palaeoclimatology, Palaeoecology 291, 456–468.

Hallam, A., Wignall, P.B., 2000. Facies changes across the Triassic–Jurassic boundary in Nevada, USA. Journal of the Geological Society 157, 49–54.

Hautmann, M., Benton, M.J., Tomašcových, A., 2008. Catastrophic ocean acidification at the Triassic–Jurassic boundary. Neues Jahrbuch für Geologie und Paläontologie 249, 119–127.

Hesselbo, S.P., Robinson, S.A., Surlyk, F., 2004. Sea-level change and facies development across potential Triassic–Jurassic boundary horizons, SW Britain. Journal of the Geological Society 161, 365–379.

Holland, S.M., 2020. The stratigraphy of mass extinctions and recoveries. Annual Review of Earth and Planetary Sciences 48, 75–97.

Larina, E., Bottjer, D.J., Corsetti, F.A., Zonneveld, J.P., Celestian, A.J., Bailey, J.V., 2019. Uppermost Triassic phosphorites from Williston Lake, Canada: link to fluctuating euxinic–anoxic conditions in northeastern Panthalassa before the end-Triassic mass extinction. Scientific Reports 9, 18790. https://doi.org/10.1038/s41598-019-55162-2.

Ikeda, M., Hori, R.S., Okada, Y., Nakada, R., 2015. Volcanism and deep-ocean acidification across the end-Triassic extinction event. Paleogeography, Paleoclimatology, Paleoecology 440, 725–733.

James, N.P., Dalrymple, R.W., 2010. Facies models 4. Geological Association of Canada, Ottowa, p. 586.

Korte, C., Ruhl, M., Pálfy, J., Ullmann, C.V., Hesselbo, S.P., 2018. Chemostratigraphy across the Triassic–Jurassic boundary. In: Sial, A.N., Gaucher, C., Ramkumar, M., Ferreira, V.P. (Eds.), Chemostratigraphy Across Major Chronological Boundaries. John Wiley & Sons, Inc., Hoboken, NJ, pp. 183–210.

Larina, E., Bottjer, D.J., Corsetti, F.A., Thibodeau, A.M., Berelson, W.M., West, J.A., Yager, J.A., 2021. Ecosystem change and carbon cycle perturbation preceded the end-Triassic mass extinction. Earth and Planetary Science Letters https://doi.org/10.1016/j.epsl.2021.117180.

Laws, R.A., 1978. Paleoecology of Late Triassic Faunas From Mineral County, Nevada and Shasta County, California. University of California, Berkeley (M.A. thesis, 149 pp.).

Laws, R.A., 1982. Late Triassic depositional environments and molluscan associations from west-central Nevada. Palaeogeography, Palaeoclimatology, Palaeoecology 37, 131–148.

Lucas, S.G., Taylor, D.G., Guex, J., Tanner, L.H., Krainer, K., 2007. Updated proposal for Global Stratotype Section and Point for the base of the Jurassic System in the New York Canyon area, Nevada, USA. International Subcommission on Jurassic Stratigraphy Newsletter 34, 34–42.

Martindale, R.C., Berelson, W.M., Corsetti, F.A., Bottjer, D.J., West, A.J., 2012. Constraining carbonate chemistry at a potential ocean acidification event (the Triassic–Jurassic boundary) using the presence of corals and coral reefs in the fossil record. Palaeogeography, Palaeoclimatology, Palaeoecology 350-352, 114–123.

Muller, S.W., Ferguson, H.G., 1936. Triassic and Lower Jurassic formations of west central Nevada. Geological Society of America Bulletin 47, 241–252.

Muller, S.W., Ferguson, H.G., 1939. Mesozoic stratigraphy of the Hawthorne and Tonopah quadrangles, Nevada. Geological Society of America Bulletin 50, 1573–1624.

Oldow, J., 1984. Evolution of a late Mesozoic back-arc fold and thrust belt, northwestern Great Basin, USA. Sedimentary Geology 102, 245–274.

Orchard, M.J., Carter, E.S., Lucas, S.G., Taylor, D.G., 2007. Rhaetian (Upper Triassic) conodonts and radiolarians from New York Canyon, Nevada, USA. Albertiana 35, 59–65.

Patzkowsky, M.E., Holland, S.M., 2012. Stratigraphic Paleobiology. University of Chicago Press, Chicago (255 pp.).

Read, J.F., 1985. Carbonate platform facies models. AAPG Bulletin 69, 1–21.

Reilly, M.B., Breyer, J.A., Oldow, J.S., 1980. Petrographic provinces and provenance of the Upper Triassic Luning Formation, west-central Nevada: summary. Geological Society of America Bulletin 91, 573–575.

Ritterbush, K.A., Bottjer, D.J., Corsetti, F.A., Rosas, S., 2014. New evidence on the role of siliceous sponges in ecology and sedimentary facies development in eastern Panthalassa following the Triassic–Jurassic mass extinction. Palaios 29, 652–668.

Ritterbush, K.A., Ibarra, Y., Tackett, L.S., 2016. Post-extinction biofacies of the first carbonate ramp of the Early Jurassic (Sinemurian) in NE Panthalassa (New York Canyon, Nevada, USA). Palaios 31, 141–160.

Rožič, B., Kolar-Jurkovšek, T., Šmuc, A., 2009. Late Triassic sedimentary evolution of Slovenian Basin (eastern Southern Alps): description and correlation of the Slatnik Formation. Facies 55, 137–155.

Ruhl, M., Kürshner, W.M., Lrystyn, L., 2009. Triassic–Jurassic organic carbon isotope stratigraphy of key section in the western Tethys realm (Austria). Earth and Planetary Science Letters 281, 169–187.

Schaltegger, U., Guex, J., Bartolini, A., Schoene, B., Ovtcharova, M., 2008. Precise U–Pb age constraints for end-Triassic mass extinction, its correlation to volcanism and Hettangian post-extinction recovery. Earth and Planetary Science Letters 267, 266–275.

Schoene, B., Guex, J., Bartolini, A., Schaltegger, U., Blackburn, T.J., 2010. Correlating the end-Triassic mass extinction and flood basalt volcanism at the 100 ka level. Geology 38, 387–390.

Silberling, N.J., Jones, D.L., 1984. Lithotectonic terrane maps of the North American Cordillera. United States Geological Survey, Open-File Report 84-523 pp. A1–D14.

Speed, R.C., 1978. Paleogeographic and plate tectonic evolution of the early Mesozoic marine province of the western Great Basin. In: Howell, D.G., McDougall, K.A. (Eds.), Mesozoic paleogeography of the western United States. Section SEPM, Los Angeles, Pacific, pp. 253–270.

Tackett, L.S., Bottjer, D.J., 2016. Paleoecological succession of Norian (Late Triassic) benthic fauna in eastern Panthalassa (Luning and Gabbs Formations, west-central Nevada). Palaios 31, 190–202.

Taylor, D.G., Smith, P.L., Laws, R.A., Guex, J., 1983. The stratigraphy and biofacies trends of the Lower Mesozoic Gabbs and Sunrise Formations, west-central Nevada. Canadian Journal of Earth Sciences 20, 1598–1608.

Taylor, D.G., Boelling, K., Guex, J., 2000. The Triassic/Jurassic system boundary in the Gabbs Formation, Nevada. GeoResearch Forum 6, 225–236.

Taylor, D., Guex, J., 2021. Early Sinemurian ammonoids and biochronology of the Sunrise Formation, New York Canyon, Mineral County, Nevada. New Mexico Museum of Natural History and Science Bulletin 82, 371–391.
Taylor, D.G., Guex, J., Lucas, S.G., 2021. Ammonoids of the latest Triassic Gabbs Formation at New York Canyon, Mineral County, Nevada. Fossil Record 7, 393–425.
Thibodeau, A.M., Ritterbush, K., Yager, J.A., West, A.J., Ibarra, Y., Bottjer, D.J., Berelson, W.M., Bergquist, B.A., Corsetti, F.A., 2016. Mercury anomalies and the timing of biotic recovery following the end-Triassic mass extinction. Nature Communications 7, 11147. https://doi.org/10.1038/ncomms11147.
Tucker, M.E., Wright, P.V., 1990. Carbonate Sedimentology. Blackwell Science Ltd., Malden, MA (482 pp.).
Tucker, M.E., Calvet, F., Hunt, D., 1993. Sequence stratigraphy of carbonate ramps: systems tracts, models and application to the Muschelkalk carbonate platforms of Eastern Spain. In: Posamentier, H.W., Summerhayes, C.P., Haq, B.U., Allen, G.P. (Eds.), Sequence Stratigraphy and Facies Associations. IAS Special Publication, vol. 18. Blackwell, Oxford, pp. 397–415.
U.S. Geological Survey, 2017. 1/3rd Arc-second Digital Elevation Models (DEMs)—USGS National Map 3DEP Downloadable Data Collection. U.S. Geological Survey.
Ward, P.D., Garrison, G.H., Haggart, J.W., Kring, D.A., Beattie, M.J., 2004. Isotopic evidence bearing on Late Triassic extinction events, Queen Charlotte Islands, British Columbia, and implications for the duration and cause of the Triassic/Jurassic mass extinction. Earth and Planetary Science Letters 224, 589–600.
Ward, P.D., Garrison, G.H., Williford, K.H., Kring, D.A., Goodwin, D.H., Beattie, M.J., McRoberts, C.A., 2007. The organic carbon isotopic and paleontological record across the Triassic–Jurassic boundary at the candidate GSSP section at Ferguson Hill, Muller Canyon, Nevada, USA. Palaeogeography, Palaeoclimatology, Palaeoecology 244, 281–289.
Wignall, P.B., Zonneveld, J.P., Newton, R.J., Amor, K., Sephton, M.A., Hartley, S., 2007. The end Triassic mass extinction record of Williston Lake, British Columbia. Palaeogeography, Palaeoclimatology, Palaeoecology 253, 385–406.
Yang, B.C., Dalrymple, R.W., Chun, S.S., 2005. Sedimentation on a wave-dominated, open-coast tidal flat, south-western Korea: summer tidal flat–winter shoreface. Sedimentology 52, 235–252.